Supporting information

t-SNARE transmembrane Domain Clustering Modulates Lipid Organization and Membrane Curvature

Satyan Sharma[†], Manfred Lindau[†§]

[†]Laboratory of Nanoscale Cell Biology, Max-Planck-Institut für biophysikalische Chemie, Göttingen, 37077 Germany;

[§]School of Applied and Engineering Physics, Cornell University, Ithaca, NY 14850, USA.

Materials and Methods

1. Protein models

The initial structure of the t-SNARE complex was taken from the X-ray structure of the cis-SNARE complex (3HD7).[1] Only the structure corresponding to residues A247-I286 of syntaxin-1 (stx1; chain B of 3HD7), A74-G82 of Synaptosomal-associated protein 25 (SNAP25-SN1; chain C of 3HD7) and A195-T200 of Synaptosomal-associated protein 25 (SNAP25-SN2; chain D of 3HD7) were kept and the rest was deleted. The missing residues 287F-288G of stx1, 83K-S98 of SNAP25-SN1 and K201-G206 of SNAP25-SN2 were modeled using Modeler[2] to generate the t-SNARE complex fragment used in this study. The t-SNARE fragment was then converted to CG using the martinize script. Distance constraints were used between layers +8 in order to keep individual t-SNARE fragments intact.

The side chains of cysteine residues C85, C88, C90 and C92 of SNAP25-SN1 were replaced with palmitoyl chains, using standard martini beads (Na-C1-C1-C1) and the connecting bond was defined with an equilibrium distance of 0.39 nm and force constant of 5000 kJ mol^{-1} nm^{-2}.[3] In the CG MARTINI force field, the cys residue is represented by two beads, one representing the main chain (BB) and with the other as its side chain (Sc). A palmitic acid (Na-C1-C1-C1-C1) is represented by one

polar bead (Na) and four other non-polar beads representing the alkyl chain (C1-C1-C1-C1). In the literature, alternative bead composition of cyp have been used and are listed here:

1. BB-C5-C1-C1-C1-C1[4]
2. BB-C5-Na-C1-C1-C1[5]
3. BB-C5-Na-C1-C1-C1-C1[6]
4. BB-Na-C1-C1-C1-C1[7]

Model 1 has a cys side chain with the alkyl chain attached to it, but represents only a thiol group (C5) and not a thioester. Model 2 includes both thiol and thioester but has a smaller alkyl chain, while Model3 combines Models 1 and 2 but has 7 beads. We have chosen Model 4, a 6-bead model used for simulation of the membrane association of AnkG that was based on the crystal structure of the s-palmitoylation region of the AnkG membrane-binding domain[7]. The Na bead was directly attached to backbone of cys using the bonded parameters of C5-Na from Model 3. This model has also been shown to better match the atomistic simulations according to the MARTINI users mailing list.

2. System preparation

Twelve copies of the t-SNARE fragment were inserted into a planar membrane via a self-assembly procedure.[8] The starting configuration of the lipids for self-assembly was generated by combing two boxes, with randomly placed intracellular leaflet (IC) lipids in one box and extracellular leaflet (EC) lipids in another. The lipids in the IC and EC boxes were placed in random orientation. Each box was 24 nm x 24 nm x 5 nm in dimension. Next, the two boxes were combined such that they overlapped by 0.5 nm along the z-axis. The lipid composition of the IC and EC boxes is shown in Table S1 (before self-assembly). Separately, the twelve copies of t-SNARE fragments were manually placed on a grid such that the minimum distance between any two beads of two neighboring t-SNARE was at least 2.0 nm. Finally, such an arrangement of t-SNAREs was inserted into the box with random IC and EC

lipids. The system was then extended on either side along the z-axis. The resulting lipids box containing the t-SNAREs and lipids was then filled with CG water and Na^+ and Cl^- ions were added to achieve a final concentration of 0.15M. Subsequently, 1000 steps of energy minimization using steepest descent algorithm and a 200 ns self-assembly run were performed. During the self-assembly, the proteins were position restrained along the x- and y- directions using a force constant of 1000 kJ mol^{-1} nm^{-2}. During this simulation, while the bilayer is forming some lipids move from one side to the other, such that the lipid bilayer self-assembles to form an asymmetric bilayer with imperfect asymmetry, as is the case in cell membranes. The composition of IC and EC leaflets after self-assembly (Table S1) retained most of the leaflet asymmetry. Such an imperfect lipid leaflet asymmetry is fully consistent with the imperfect lipid asymmetry in cell membranes [9]. The asymmetry obtained at the end of the self-assembly was independent of the presence of the t-SNAREs in the simulation (Figure S1). Next, the restrains were removed and the system was simulated three times (5 μs each) with different random initial velocities. The average cholesterol distributions in the IC and EC leaflets were ~38% and 45%, respectively, with the remaining cholesterol located in the hydrophobic center between the two leaflets. Cholesterol molecules show dynamic flip-flop behavior. We calculated the number of flips and flops from IC to EC leaflet and EC to IC leaflet, respectively over 100 ns intervals. For this, the entire 5 μs trajectory from all the three simulations was considered (15 μs in total). The average the number of flip-flops in a 100 ns time interval was 368 ± 23, and did not change over the duration of the simulation. With a total number of 439 cholesterol molecules present in the system, this corresponds to a flip-flop rate constant of 368/439 per 100 ns or $8.38 \pm 0.006 \times 10^6$ s^{-1}

3. Simulation details

All simulations were run using version 4.6.5 of Gromacs[10] and the MARTINI force-field ver 2.1.[11] Self-assembly was performed by using the Berendsen weak coupling thermostat (310K) and a semi-

isotropic pressure coupling with barostat (1 bar) algorithms[12] with coupling constants of 1.0 ps and 3.0 ps. After self-assembly, the temperature was kept constant at 310K using the v-rescale algorithm[13] with a time constant of 1.0 ps and Parrinello-Rahman algorithm[14] for semi-isotropic pressure coupling with a time constant of 10.0 ps. Non-bonded interactions were accounted for using a shift function with a coulomb cutoff of 1.2 nm and Van der Waals potential were smoothly shifted to zero between 0.9 and 1.2 nm. The neighbor list was updated every 10 steps with a cutoff of 1.4 nm.

4. Analysis

All visualizations were done with VMD.[15] Analyses were done using GROMACS routines and in-house scripts. For clustering, two t-SNAREs were considered to be in a cluster when any of their beads were found within 0.6 nm of each other. The inter-t-SNARE contacts were analyzed for Sim1, Sim2 and Sim3, by concatenating the last 500 ns of the three trajectories. The number of contacts between the backbone beads of t-SNARE fragment pairs was calculated with a cut-off of 0.75 nm for all possible combinations of the twelve t-SNARE fragments present in the system. The total number of contacts were then averaged over all the frames and normalized by a factor F (=66), describing probability of randomly choosing two t-SNAREs molecules out of twelve t-SNAREs.

Lipid enrichment analysis was done separately for the IC and EC leaflets. The first tail bead of the phospholipids (AM1 and GL1) and cholesterol head group (ROH) was used as the reference beads for locating the position of lipids. A cholesterol was assigned to a leaflet when its reference bead was found within 0.8 nm from the nearest phospholipid reference bead along the z-axis. The cholesterol further away than 0.8 nm were considered to be in the bilayer core and not included in the analysis. For each frame, lipid composition was analyzed within 0.8 nm of protein for each leaflet and the numbers of each lipid were compared to its number frequency in the corresponding leaflet. The results are shown as average over all the frames. Cholesterol enrichment in the membrane leaflets was calculated

using a procedure similar to one described previously.[16] On each leaflet a 2D Voronoi analysis was carried out using the x and y coordinates of reference beads and the cholesterol enrichment was calculated, as described above, using lipid neighbors of each Voronoi cell.

To ascertain the number of cholesterol flip-flops over the entire simulations Sim1 to Sim3, a cholesterol was assigned to a leaflet, if its ROH bead was found within the 0.8 nm along the z-axis from the center of mass of the phospholipid reference beads in the respective IC or EC leaflets along the z-axis. A flip was counted only if the ROH bead moved from one leaflet to reach within 0.8 nm of the other leaflet. The same leaflet assignment was also used to estimate the number of cholesterol in the individual leaflets during the simulation trajectory.

The membrane curvature was analyzed using a rolling circle method. At first, the membrane was divided into 1 nm x 1nm vertical square prisms. The coordinates of all lipid tail beads and the TMD of stx1 form 50 frames over last 20 ns were combined to describe the membrane. Within each square prism, the center of mass (com) of the all lipid tail beads and the TMD of stx1 were averaged to obtain an approximate membrane surface. The radius of the principal curvature along the x-axis was calculated by fitting a circle at each point on individual x-z planes perpendicular to y-axes. For each point on a given x-z plane, a circle was fitted using four adjacent points on either side, thus defining a ~9 nm arc length for fitting. If the center of the fitted circle was located below the z-value of the point, the radius was assigned a positive value, if it was above the point it was assigned a negative curvature, consistent with the assignment of positive curvature to indicate regions of membrane that curve inwards towards the cytoplasm.[17] The procedure was repeated for all points. The principal curvature along x-axis is then given by the inverse of the radius of the fitted circle at each point. Similarly, the principal curvature along y-axis was calculated at each point lying on different y-z planes. The total curvature at a point is the sum of the two curvatures at that point along the x- and y- axes.

The second-rank lipid order parameter P_2 was computed between tail bead 2 and tail bead 3 using the equation

$$P_2 = \frac{1}{2}(3\langle cos^2\,\theta\rangle - 1),$$

where θ is the angle between the bond connecting the tail beads 2 and 3 and the bilayer normal.[16] The order parameter was calculated using an in-house python script and plotted using *dispgrid.py*. [18]

Table S1: Lipid composition of the plasma membrane of smaller sized system.

Lipids			Before self-assembly (%)		After self-assembly (%)	
sn-1	sn-2	Count	IC leaflet	EC leaflet	IC leaflet	EC leaflet
Phosphatidylcholine (PC)		**(41)**[a]	**(0.0)**[b]	**(100.0)**[b]	**(19.2)**[b]	**(80.8)**[b]
16:0/18:0	16:0/18:0	168	0	100	18.5	81.5
16:0/18:0	18:1	187	0	100	18.7	81.3
16:0/18:0	20:4/22:4	38	0	100	28.9	71.1
16:0/18:0	22:5/22:6	23	0	100	13.0	87.0
Phosphatidylethanolamine (PE)		**(34)**	**(100.0)**	**(0.0)**	**(74.3)**	**(25.7)**
16:0/18:0	18:1	54	100	0	81.5	18.5
16:0/18:0	20:4/22:4	144	100	0	69.4	30.6
16:0/18:0	22:5/22:6	55	100	0	70.9	29.1
22:5/22:6	22:5/22:6	89	100	0	79.8	20.2
Phosphatidylserine (PS)		**(13)**	**(100.0)**	**(0.0)**	**(79.8)**	**(20.2)**
16:0/18:0	18:1	20	100	0	65.0	35.0
16:0/18:0	20:4/22:4	15	100	0	80.0	20.0
16:0/18:0	22:5/22:6	97	100	0	56.7	43.3
Sphingomyelin (SM)		**(5)**	**(0.0)**	**(100.0)**	**(27.5)**	**(72.5)**
16:0/18:0	16:0/18:0	46	0	100	28.3	71.7
16:0/18:0	23:1/24:1	3	0	100	33.3	66.7
20:0/22:0	20:0/22:0	1	0	100	0.0	100.0
24:0	24:0	1	0	100	0.0	100.0
Phosphatidylinositol (PI)		**(3)**	**(1000.0)**	**(0.0)**	**(77.1)**	**(22.9)**
16:0/18:0	18:1	6	100	0	83.3	16.7
16:0/18:0	20:4/22:4	26	100	0	80.8	19.2
16:0/18:0	22:5/22:6	3	100	0	33.3	66.7
Glycolipid 1 (GM1)		**(2)**	**(0.0)**	**(100.0)**	**(25.0)**	**(75.0)**
16:0/18:0	16:0/18:0	20	0	100	25.0	75.0
Glycolipid 3 (GM3)		**(2)**	**(0.0)**	**(100.0)**	**(10.0)**	**(90.0)**
16:0/18:0	16:0/18:0	20	0	100	10.0	90.0
Cholesterol		**(43)**				
		439	37.5	62.5	37.9[c]	45.1[c]

(a) Percentage of each class of lipid with respect to the total phospholipids in the bilayer.
(b) Percentage asymmetry of each class of lipid in the bilayer.
(c) Average cholesterol distribution in the leaflet from 15 μs (Sim1to3, each 5 μs). Of 439 cholesterol molecules, 166.41 ± 11.03 were in IC leaflet, 198 ± 11.21 were in EC leaflet and 74.46 ± 18.72 were located in membrane interior.

(a)

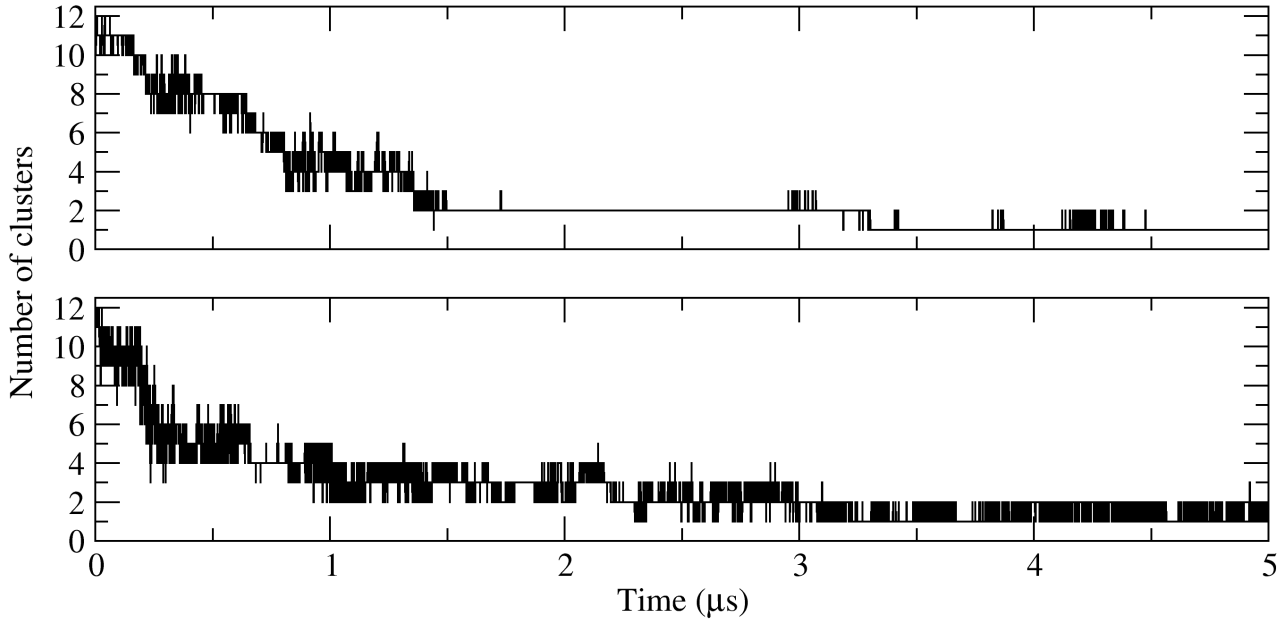

(b)

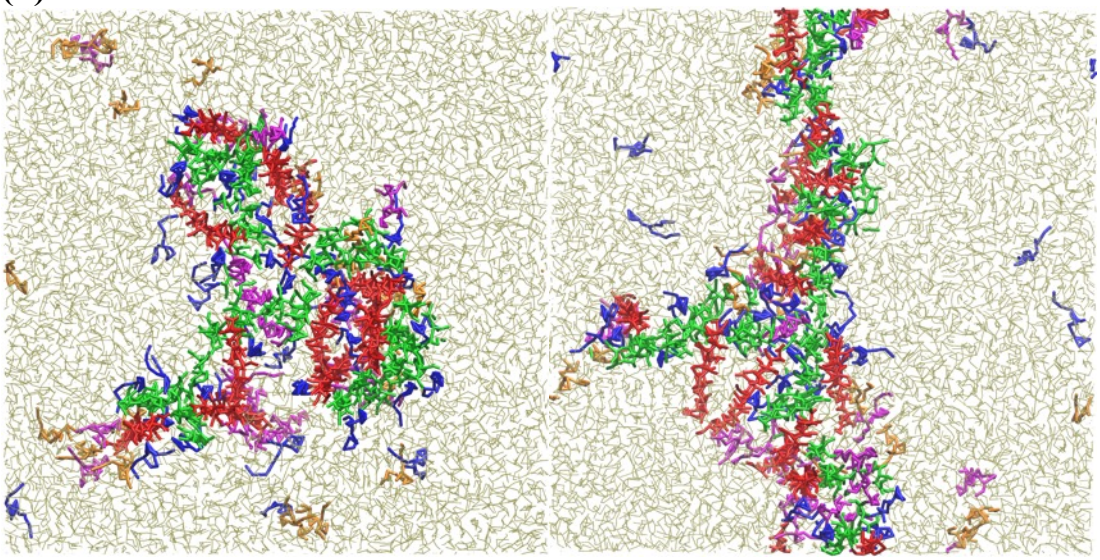

Figure S1. (a) Evolution of number of t-SNARE clusters from the simulations Sim2 (upper panel) and Sim3 (lower panel). (b) Snapshot at 5 μs for the simulations, Sim2 (left panel) and Sim3 (right panel), showing the t-SNARE clusters (stx1 red; SNAP25 green). Also shown are the PIP2 (blue), GM1 (magenta) and GM3 (orange) lipids.

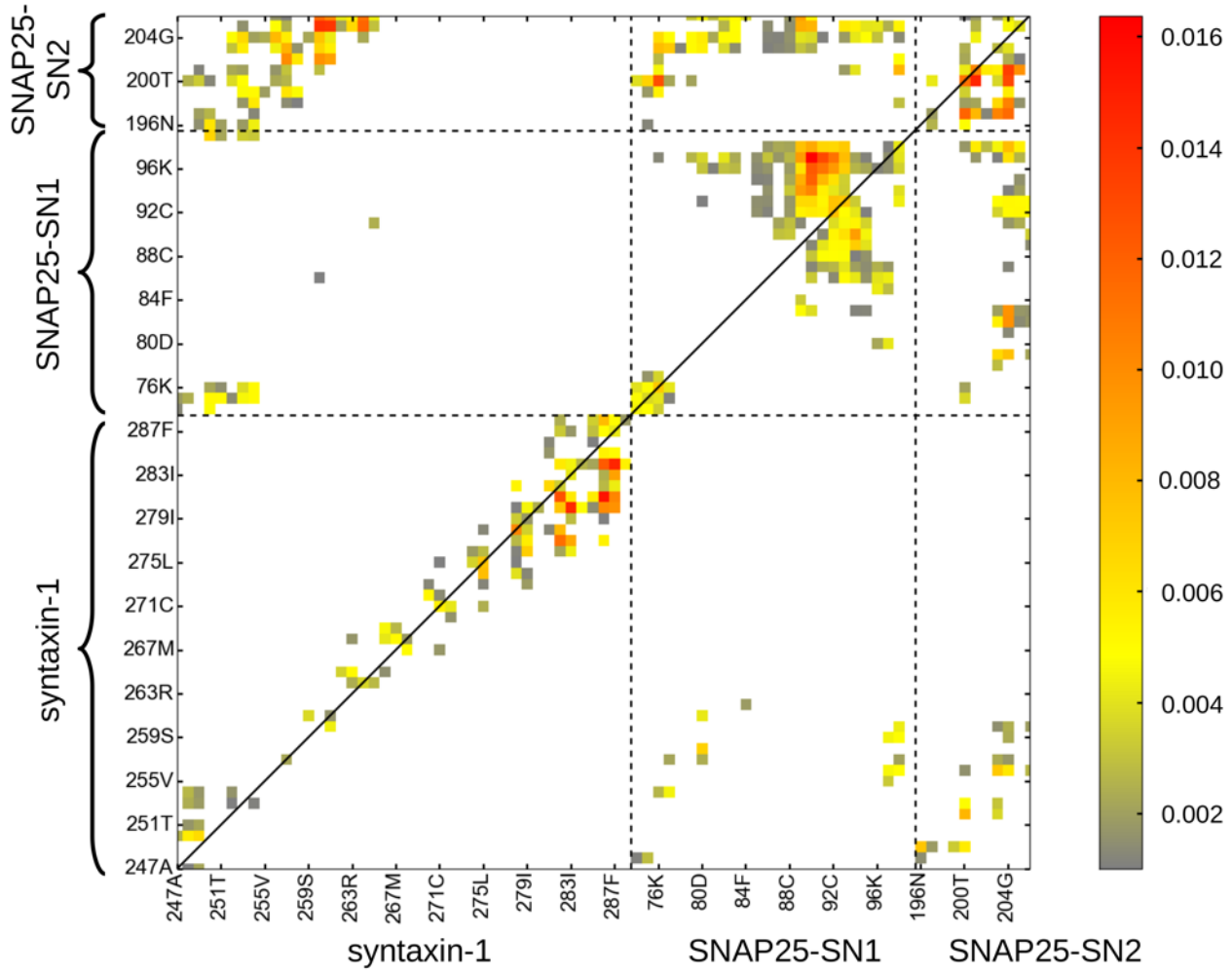

Figure S2. Inter-t-SNARE residue contact probability map over last 500 ns of all the three simulations with 12 copies of t-SNAREs.

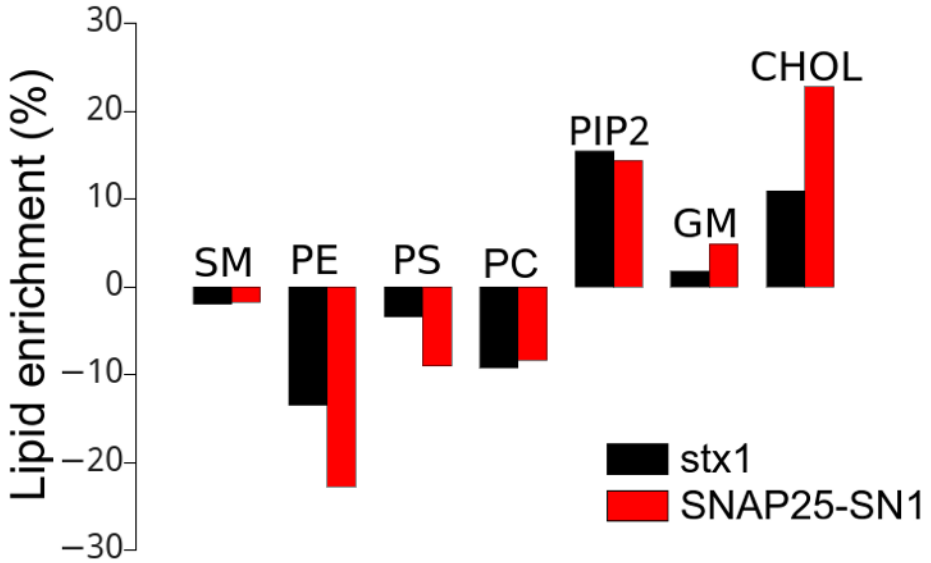

Figure S3. Analysis of lipid enrichment within 0.8 nm of syntaxin-1 (black) and SNAP25-SN1 (red) at the intracellular leaflet, averaged over all the three simulations Sim1 to Sim3.

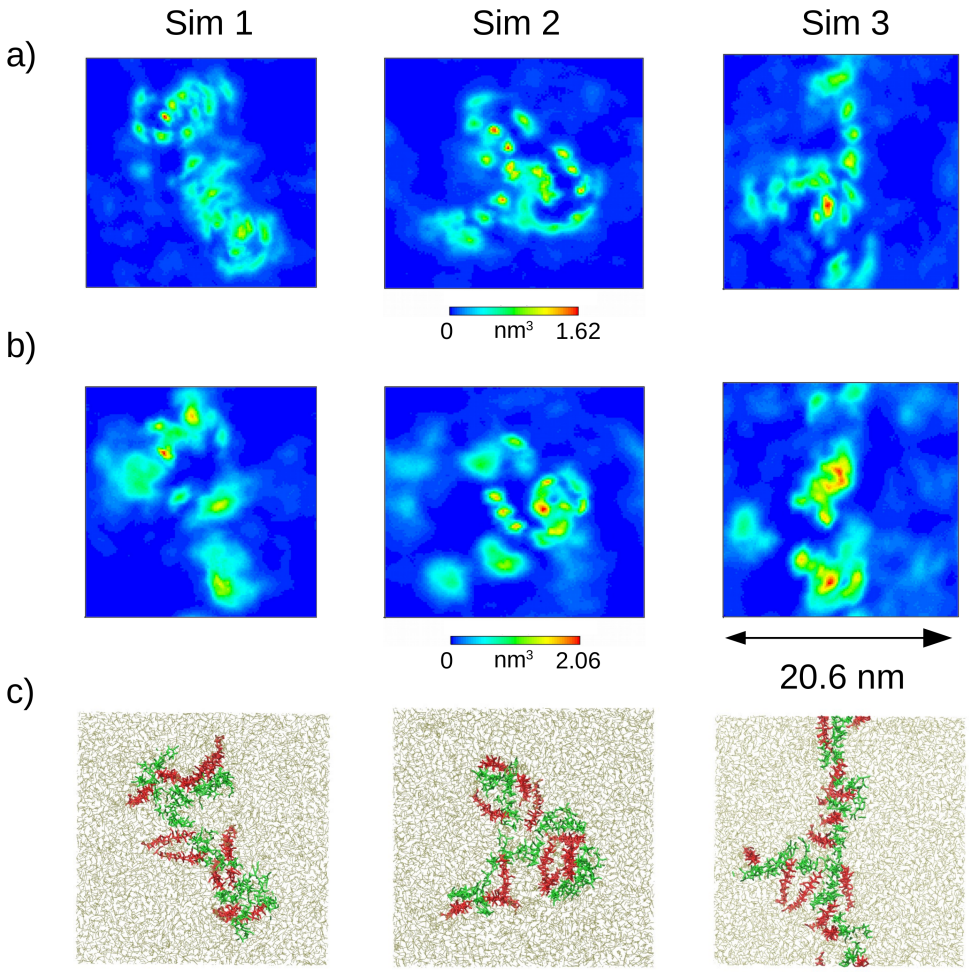

Figure S4. 2D number densities of (a) PIP2 and (b) GM (lower panel) from the last 500 ns of the three simulations (Sim1, Sim2 and Sim3). (c) Orientation of the t-SNARE clusters (stx1 red; SNAP25 green) from the snapshot at 5 μs form the three simulations. The membrane lipids are shown in brown.

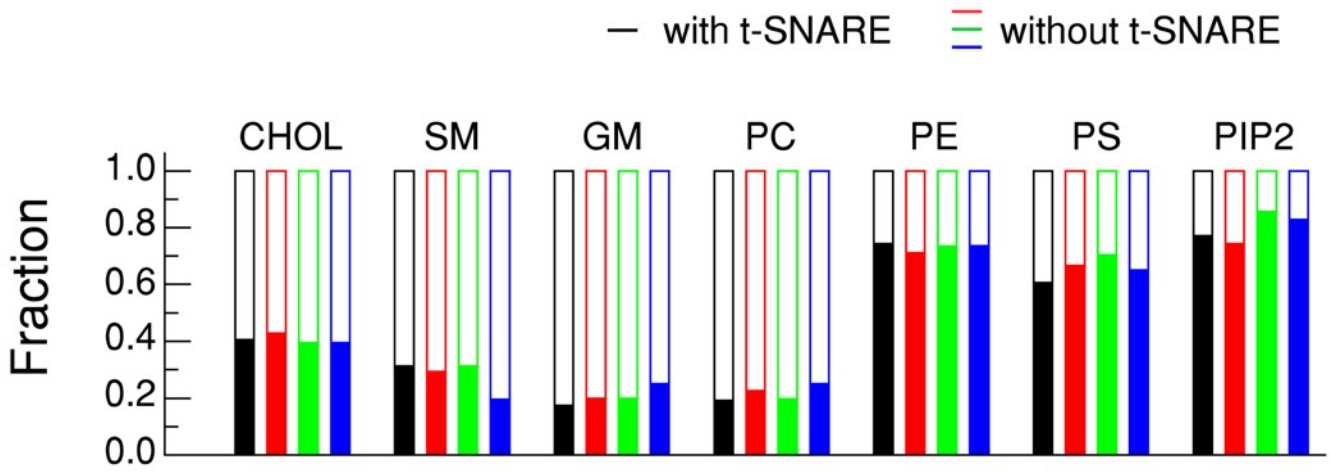

Figure S5. Lipid asymmetry of a self-assembly simulation in the presence of t-SNARE TMDs (black) or three independent self-assembly simulations in the absence of t-SNARE TMDs (red, green and blue). The asymmetry was calculated as a ratio of the number of each lipid species in either leaflet to its total number in the membrane. The asymmetry was calculated from a snapshot at 200 ns, at the end of the self-assembly simulation. The fractions of different lipid classes in the EC leaflet (open bars) and in the IC leaflet (solid bars). In the absence of t-SNAREs the variation in lipid leaflet distribution percentages between individual simulations was < 12% for all the different lipid species. The distribution percentage values in the presence of t-SNAREs (black bars) for all lipids were close to those obtained in the absence of t-SNAREs (colored bars).

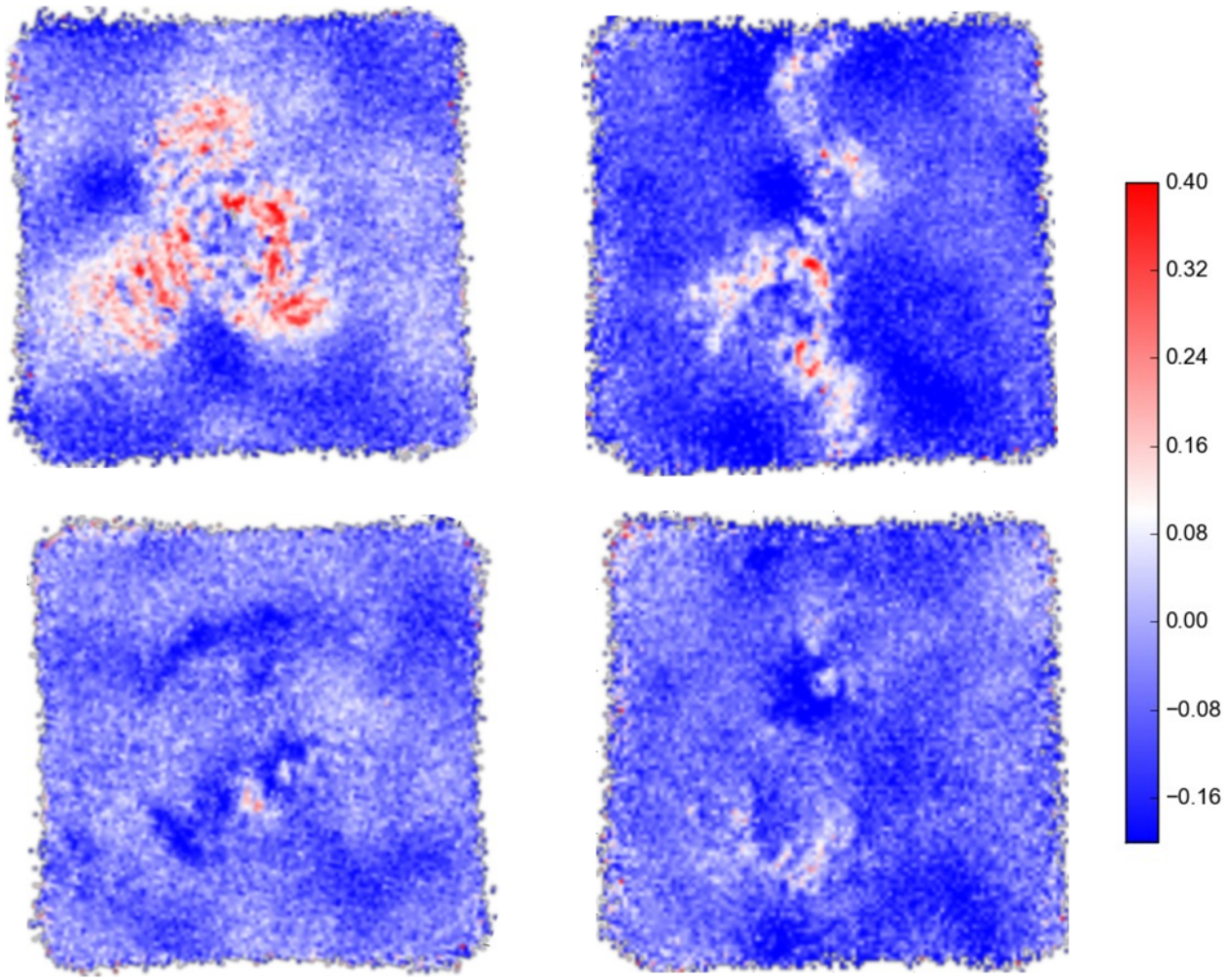

Figure S6. Cholesterol enrichment at the IC leaflet (top panels) and EC leaflet (bottom panels) for Sim2 (left panels) and Sim3 (right panels).

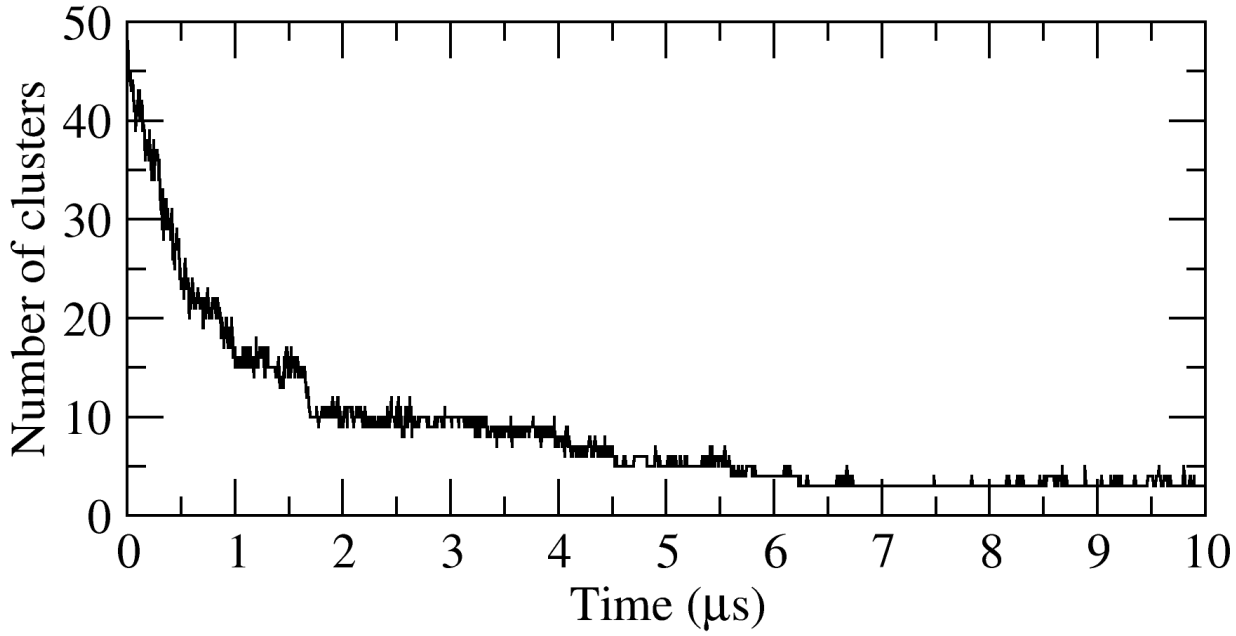

Figure S7. Evolution of number of t-SNARE clusters for the bigger system (SimL1).

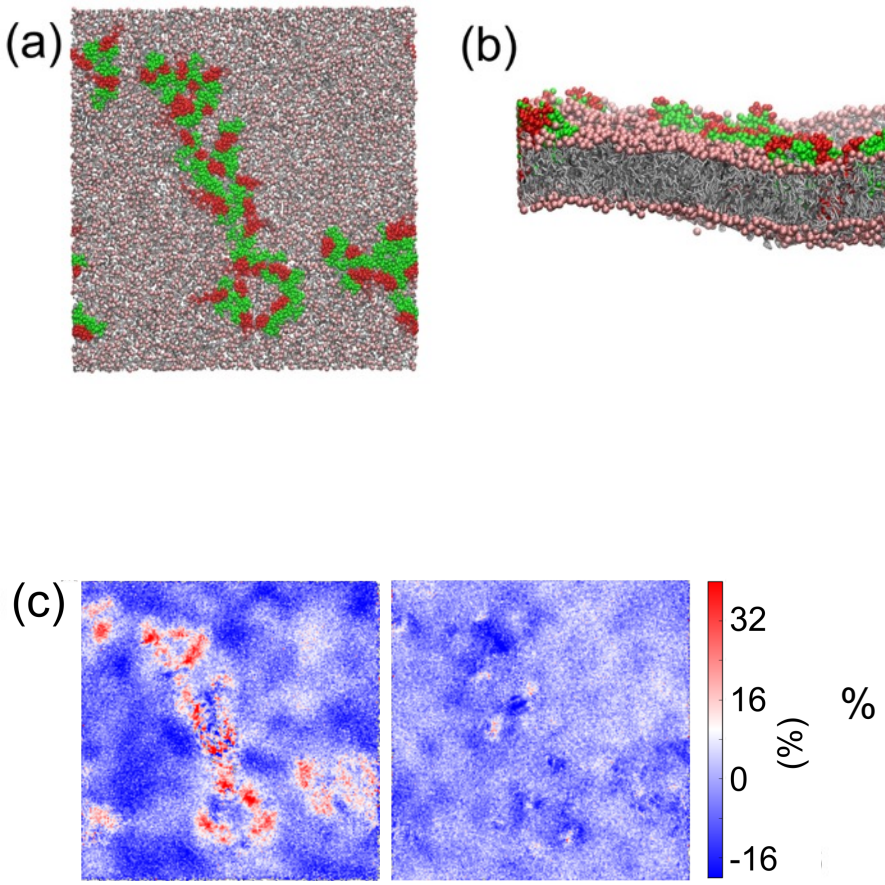

Figure S8. (a) Snapshot at 10 μs showing t-SNARE clusters (stx1 red, SNAP25 green). (b) A side-view of the system at 10 μs showing the membrane curvature for SimL1. (c) Cholesterol enrichment at the IC leaflet (top panels) and EC leaflet (bottom panels) for SimL1.

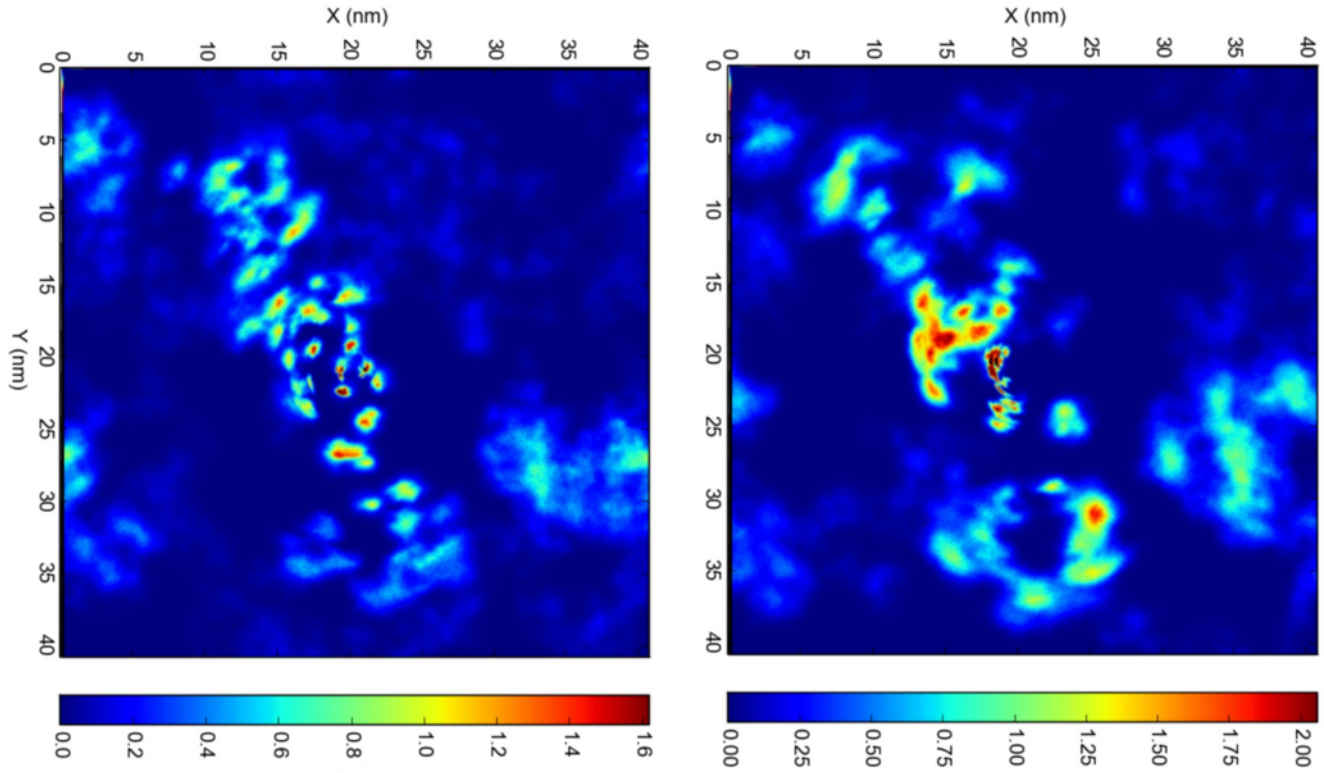

Figure S9. 2D number densities of PIP2 (right panel) and GM (left panel), analyzed over the last 200 ns of the simulation of the larger system (SimL1).

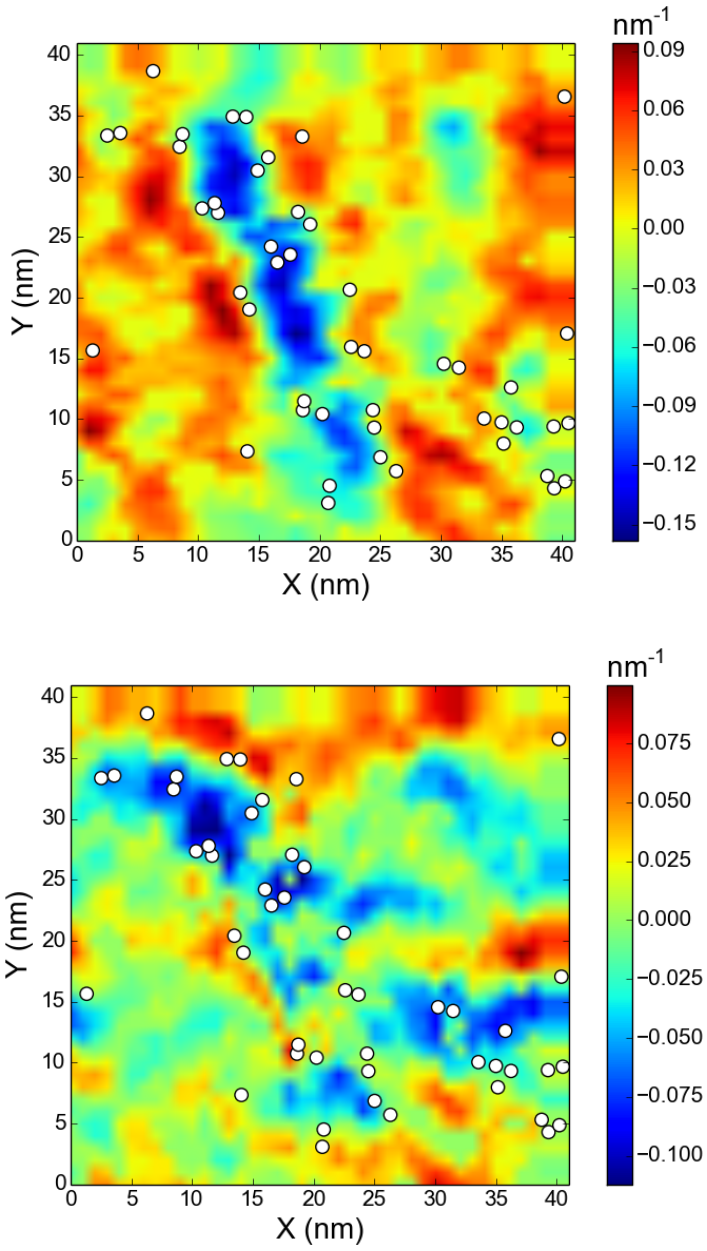

Figure S10. The principal curvatures of the membrane along x- (top) and y- (bottom) axes for simL1. Each plot shows the curvature calculated for the averaged membrane surface obtained from 50 frames over the last 20 ns of the simulation.

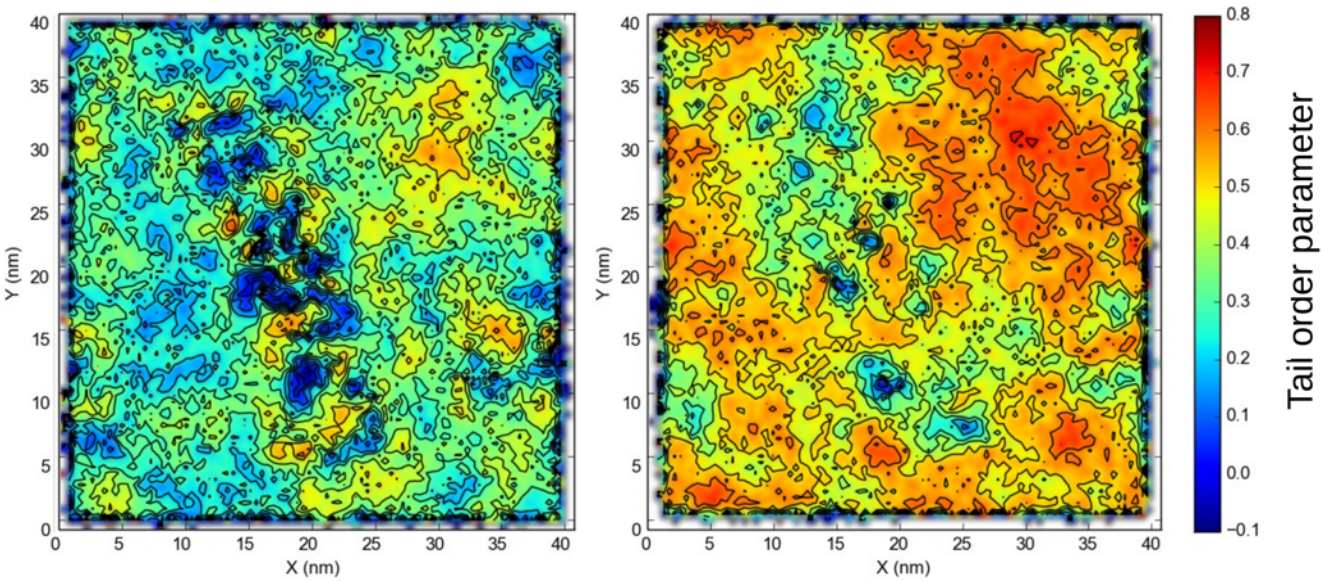

Figure S11. Membrane order parameter for IC leaflet (left panel) and EC leaflet (right panel) from the last 200 ns of SimL1. The tail order parameters were evaluated between tail bead 2 and tail bead 3 for all phospholipids.

Supporting Information References:

1. Stein, A.; Weber, G.; Wahl, M. C.; Jahn, R., *Nature* **2009,** *460* (7254), 525-8.

2. Sali, A.; Blundell, T. L., *J Mol Biol* **1993,** *234* (3), 779-815.

3. de Jong, D. H.; Lopez, C. A.; Marrink, S. J., *Faraday Discuss* **2012,** *161*, 347-63.

4. Johnston, J. M.; Filizola, M., *PLoS One* **2014,** *9* (2), e90694.

5. Li, Z.; Janosi, L.; Gorfe, A. A., *J Am Chem Soc* **2012,** *134* (41), 17278-85.

6. de Jong, D. H.; Lopez, C. A.; Marrink, S. J., *Faraday Discuss.* **2013,** *161*, 347-63.

7. Fujiwara, Y.; Kondo, H. X.; Shirota, M.; Kobayashi, M.; Takeshita, K.; Nakagawa, A.; Okamura, Y.; Kinoshita, K., *Sci Rep* **2016,** *6*, 23981.

8. Sharma, S.; Kim, B. N.; Stansfeld, P. J.; Sansom, M. S.; Lindau, M., *PLoS One* **2015,** *10* (12), e0144814.

9. Fujimoto, T.; Parmryd, I., *Front Cell Dev Biol* **2016,** *4*, 155.

10. Hess, B.; Kutzner, C.; van der Spoel, D.; Lindahl, E., *J Chem Theory Comput* **2008,** *4* (3), 435-47.

11. Marrink, S. J.; Risselada, H. J.; Yefimov, S.; Tieleman, D. P.; de Vries, A. H., *J Phys Chem B* **2007,** *111* (27), 7812-24.

12. Berendsen, H. J. C.; Postma, J. P. M.; Vangunsteren, W. F.; Dinola, A.; Haak, J. R., *J. Chem. Phys.* **1984,** *81* (8), 3684-3690.

13. Bussi, G.; Donadio, D.; Parrinello, M., *J Chem Phys* **2007,** *126* (1), 014101.

14. Parrinello, M.; Rahman, A., *J. Appl. Phys.* **1981,** *52* (12), 7182-7190.

15. Humphrey, W.; Dalke, A.; Schulten, K., *J Mol Graph* **1996,** *14* (1), 33-8, 27-8.

16. Ingolfsson, H. I.; Melo, M. N.; van Eerden, F. J.; Arnarez, C.; Lopez, C. A.; Wassenaar, T. A.; Periole, X.; de Vries, A. H.; Tieleman, D. P.; Marrink, S. J., *J Am Chem Soc* **2014,** *136* (41), 14554-9.

17. McMahon, H. T.; Gallop, J. L., *Nature* **2005,** *438* (7068), 590-6.

18. Castillo, N.; Monticelli, L.; Barnoud, J.; Tieleman, D. P., *Chem Phys Lipids* **2013,** *169*, 95-105.